ELSEVIER

Thermochimica Acta 248 (1995) 147–160

thermochimica acta

Thermal analysis of chiral drug mixtures: the DSC behavior of mixtures of ephedrine HCl and pseudoephedrine HCl enantiomers

R.J. Prankerd [a,*], M.Z. Elsabee [b]

[a] *Department of Pharmacy, University of Queensland, St. Lucia, Brisbane, QLD 4072, Australia*
[b] *Department of Chemistry, University of Cairo, Cairo, Egypt*

Received 24 September 1993; accepted 30 November 1993

Abstract

A method for peak shape analysis and deconvolution of overlapping endotherms in differential scanning calorimetry (DSC) data has been previously reported. In this study the method is applied to binary mixtures of, (i) (1S,2S)-(+)- and (1R,2R)-(−)-Ψ-ephedrine HCl, and (ii) (1S,2S)-(+)-Ψ-ephedrine HCl and its diastereomer, (1S,2R)-(+)-ephedrine HCl. Phase diagrams based on enthalpies of fusion at the melting point (ΔH_f^m) as a function of mol% composition are linear. However, the phase diagrams based on melting temperature as a function of mol% composition are non-linear and show deviations from the theoretical Prigogine–Defay and Schröder–van Laar equations. Estimates of eutectic compositions are more definitive from the diagrams based on ΔH_f^m values. The phase diagram for the Ψ-ephedrine HCl enantiomers demonstrates racemic compound formation with eutectic points for the compound and the pure enantiomers at 28.1 ± 2.5 mol% and 71.9 ± 2.5 mol%. The ΔH_f^m phase diagram for mixtures of (1S,2R)-(+)-ephedrine HCl and (1S,2S)-(+)-Ψ-ephedrine HCl suggested the formation of a weak complex with a composition close to 60 mol% of the (1S,2S)-(+)-isomer.

Keywords: Binary system; DSC; Enantiomer; Ephedrine; Eutectic; Heat of fusion

* Corresponding author.

SSDI 0040-6031(94)01885-K

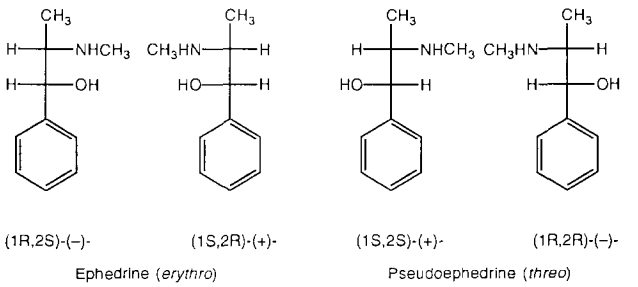

Scheme 1. Erythro and threo configurations of the 1-phenyl-2-aminomethylpropanol structure.

1. Introduction

The presence of two asymmetric carbon atoms in the 1-phenyl-2-aminomethylpropanol structure leads to the formation of two diastereomeric pairs, ephedrine and Ψ-ephedrine, each with two enantiomers. Diastereomers are optical isomers which are not mirror images of each other, and thus have differing physicochemical as well as stereoptical properties. The diastereomers of ephedrine and Ψ-ephedrine exist in the erythro and threo forms (Scheme 1).

From infrared (IR) spectroscopic studies in solution [1], it was suggested that the free base form of Ψ-ephedrine formed stronger intramolecular hydrogen bonds than did ephedrine. Nuclear magnetic resonance (NMR) studies have provided additional evidence that Ψ-ephedrine free base has stronger intramolecular hydrogen bonds and that ephedrine and Ψ-ephedrine occur in "off staggered" conformations [2,3]. NMR coupling constant comparisons with the rotationally more restricted 3-methyl-2-phenylmorpholine diastereomers supported the intramolecular hydrogen bond hypothesis for both the free bases and the salts of ephedrine and Ψ-ephedrine in solution [4]. However, X-ray diffraction studies showed that intramolecular hydrogen bonding did not occur in the solid state for either (−)-ephedrine HCl [5] or in (1S,2S)-(+)-Ψ-ephedrine HCl [6]. In each case, pairs of organic cations were hydrogen bonded to pairs of chloride ions. Each cation contributed one N–H and one O–H hydrogen bond to one chloride ion and one N–H hydrogen bond to the other (bifurcated hydrogen bonds). Furthermore, evidence was weak for an intramolecular hydrogen bond in solid (1S,2S)-(+)-Ψ-ephedrine free base [6].

Reports have pointed to significant differences in physical and biological properties of the four 1-phenyl-2-aminomethylpropanol stereoisomers [7]. Because enantiomers and racemates frequently exhibit differences in biological activity due to qualitative or quantitative structure–activity differences in the enantiomers, new methods for determination of the optical purity of chiral drugs have gained increasing importance. Recently, we have proposed that differential scanning calorimetry (DSC) could be used qualitatively to detect chiral impurities and to quantify the minor component in binary mixtures of optical antipodes [8,9]. In the case of R-(+)- and S-(−)-propranolol hydrochloride, it was possible to quantify from 2–15 mol% of one component in the presence of 98–85 mol% of the other, by comparing the

asymmetry of its high temperature melting endotherm with a linear calibration plot of asymmetry versus composition [9]. A single calibration plot was obtained irrespective of whether the R-(+) or the S-(−) enantiomer was in excess, as expected.

Virtually all previous work on the solid–liquid phase diagrams of chiral drugs has depended on analyses of the relationships between melting temperature and composition. These are non-linear relationships, which are described for chiral mixtures by either the Prigogine–Defay [10] or Schröder–van Laar [11,12] equations (Appendix). Thermodynamic functions for the fusion of enantiomeric mixtures are not usually reported due to extensive overlap of the endotherms for fusion of the eutectic and the pure enantiomer in excess or the eutectic and the 1:1 racemic compound (complex). We have previously reported a method for deconvolution of overlapping endotherms in DSC heat flux versus temperature data, which allows the use of enthalpies of fusion at the melting point (ΔH_f^m) in correlations with composition [8,9]. The method involves fitting the DSC heat flux–temperature data to simultaneous multiple non-linear regression equations. Symmetrical endotherms are fitted to a gaussian distribution

$$y = a_0 \exp\left[\frac{-z^2}{2}\right] \tag{1}$$

where y is the measured heat flux for each temperature point on the DSC scan, a_0 is the peak amplitude and z is a scaled representation of the x value as defined in

$$z = \frac{x - a_1}{a_2} \tag{2}$$

where x is the temperature for each flux measurement, a_1 is the value of x corresponding to the peak center and a_2 is the standard deviation. Asymmetric endotherms are fitted to an exponentially modified gaussian distribution

$$y = f(x) = a_0 \exp\left[\frac{a_2^2}{2a_3^2} + \frac{a_1 - x}{a_3}\right]\left[\operatorname{erf}\left\{\frac{x - a_1}{\sqrt{2}a_2} - \frac{a_2}{\sqrt{2}a_3}\right\} + 1\right] \tag{3}$$

where the peak area $= 2a_0a_3$, a_3 is an asymmetry factor and erf{ } is an error function.

For all examples studied so far, there was a linear relationship between ΔH_f^m and mol% composition. In a previous paper [8], the solid–liquid phase diagram of (1R,2S)(−)- and (1S,2R)(+)-ephedrine HCl was investigated. It was shown, as expected, that physical mixtures of the two enantiomers form a simple eutectic (i.e. a racemic mixture) with a 1:1 ratio. In the present study, the thermal behavior of (1S,2S)(+)- and (1R,2R)(−)-Ψ-ephedrine HCl mixtures, and also mixtures of (1S,2S)(+)-Ψ-ephedrine HCl with (1S,2R)(+)-ephedrine HCl has been investigated.

2. Materials and methods

The (1S,2S)-(+) and (1R,2R)-(−) enantiomers of Ψ-ephedrine HCl and (1S,2R)-(+)-ephedrine HCl were used as received (99%, Aldrich, Milwaukee, WI).

Finely powdered physical mixtures of each pair of isomers were prepared in various compositions by very thorough grinding for at least 5 min using an agate mortar and pestle of accurately weighed quantities of each isomer (Cahn Model 2000 electromicrobalance). DSC scans of 2–4 mg of each mixture in hermetically sealed aluminum pans were obtained at a heating rate of 2.0 K min^{-1} with a Perkin-Elmer DSC-7 instrument controlled by an IBM PS/2 Model 50 Z microcomputer [8]. Values for ΔH_f^m were obtained for the total area under each scan, using the DSC-7 software. Deconvolution of the DSC endotherms was performed with Peakfit® (Version 2.0, Jandel Scientific, Corte Madera, CA), as previously described [8,9]. IR spectra were obtained for 1–2 mg of the ground binary mixtures gently dispersed in preground potassium bromide (KBr, 100 mg, Fisher, IR grade) and compressed in a 13 mm stainless steel die at 5000 lbf in^{-2} (Carver Laboratory Press, Fred S. Carver, Inc., Summit, NJ). Spectra were recorded with a Perkin-Elmer 1600 Fourier transform (FT) spectrophotometer, using 16 scans for each sample. The spectra were corrected by subtracting the spectrum of a blank KBr pellet of equal mass.

3. Results and discussion

3.1. Binary phase diagram of (1S,2S)-(+)- and (1R,2R)-(−)-Ψ-ephedrine HCl

The DSC scan of pure (1R,2R)-(−)-Ψ-ephedrine HCl displayed a single endotherm with $\Delta H_f^m = 139.48$ J g^{-1} and a liquidus temperature of 183.8°C. On physical mixing with 2.61 mol% of the (1S,2S)-(+) enantiomer, a second endotherm resulted, indicating the formation of a eutectic which melted at a lower temperature (159°C). This endotherm was about 5% of the area of the principal endotherm, indicating that it could probably be detected after the addition of only 1 mol% of the minor component. This supports the results of earlier studies [8,9], which show that DSC can detect very minor contamination of a chiral substance by its optical antipode.

This finding is of some utility, as resolution of a diastereomeric salt or drug by recrystallization to constant optical rotation requires an independent standard of 100% chiral purity, or an alternative method of chiral discrimination to be sure that resolution is complete. A study which claimed recrystallization of the diastereomeric salts of a chiral barbituric acid derivative to "constant (optical) rotation" [13], was subsequently shown to have resulted in markedly incomplete resolution when the target compounds were synthesized from pure chiral starting materials [14]. Examination by DSC of such an incompletely resolved mixture would still be expected to exhibit more than one melting endotherm, demonstrating the presence of the chiral impurity, even without diastereomeric salt formation. Allusion has recently been made to some of the requirements of chiral high performance liquid chromatography in order to quantitate low levels of enantiomeric impurities, and the physicochemical consequences of the presence of such impurities in crystals of (−)-ephedrinium 2-naphthalenesulfonate [15,16]. It was shown that enantiomeric impurities were adsorbed onto the surface of the crystals and also incorporated

within the crystal lattice [16]. The ability to economically and rapidly detect/quantitate chiral impurities by the DSC method reported here and elsewhere [8,9] may be of much value in the manufacture, formulation and regulation of new chiral drug substances.

With increasing mol% of the (1S,2S)-(+) enantiomer in the mixture, the ΔH_f^m value for the low-melting endotherm increased, as seen in Table 1. The higher temperature endotherm became increasingly broad, and the two endotherms began to overlap after the addition of 7–8 mol% of the minor component. Evaluation of the enthalpies of fusion of each individual component required deconvolution of the endotherms. When the ratio of the minor component increased to 29 mol%, the two

Table 1
Enthalpies of fusion and liquidus temperatures as a function of composition for the system (1S,2S)-(+)- and (1R,2R)-(−)-Ψ-ephedrine HCl

(1S,2S)-(+)-Ψ-ephedrine HCl/ mol%	$\Delta H_f^m(1)$/J g^{-1}	$\Delta H_f^m(2)$/J g^{-1}	Liquidus temperature/ °C
0.00	–	139.3	183.8
2.61	6.90	127.3	183.1
7.85	28.96	100.7	179.3
9.66	36.43	85.73	178.4
14.24	50.05	84.27	177.3
16.87	61.87	65.87	173.0
19.88	77.89	60.47	172.0
25.78	97.97	31.05	167.6
29.81	81.76	46.60	163.3
30.64	84.60	46.64	
32.93	67.96	57.14	164.4
37.04	60.00	75.05	162.5
40.78	41.30	92.09	162.5
41.86	39.43	85.09	163.5
45.57	43.00	88.60	163.5
46.35	36.46	101.5	164.2
49.95	10.41	122.2	164.5
55.58	44.84	84.79	163.3
57.24	44.80	88.85	163.8
57.54	50.87	81.24	162.5
59.76	54.31	76.05	162.4
64.80	–	–	164.8
64.86	78.31	54.60	162.3
68.84	93.87	36.04	164.0
70.12	82.90	51.10	166.9
75.06	85.92	51.07	168.8
79.00	76.39	58.64	171.7
85.21	49.08	89.72	175.9
90.94	28.80	103.1	178.1
96.10	15.00	124.0	180.3
96.87	6.80	130.2	181.0
100.0	–	136.6	184.5

endotherms coalesced into a single peak with a very broad base, which could still be deconvoluted into two endotherms. At about 40 mol%, the endotherms began to separate. At 50% composition, a single broad endotherm was obtained, provided that grinding was very thorough, otherwise a second minor endotherm also resulted. Fig. 1 shows representative examples of the deconvoluted endotherms.

The plot of liquidus temperature versus composition for this system differs from the racemic mixture phase diagram previously reported for (1R,2S)-(−)- and

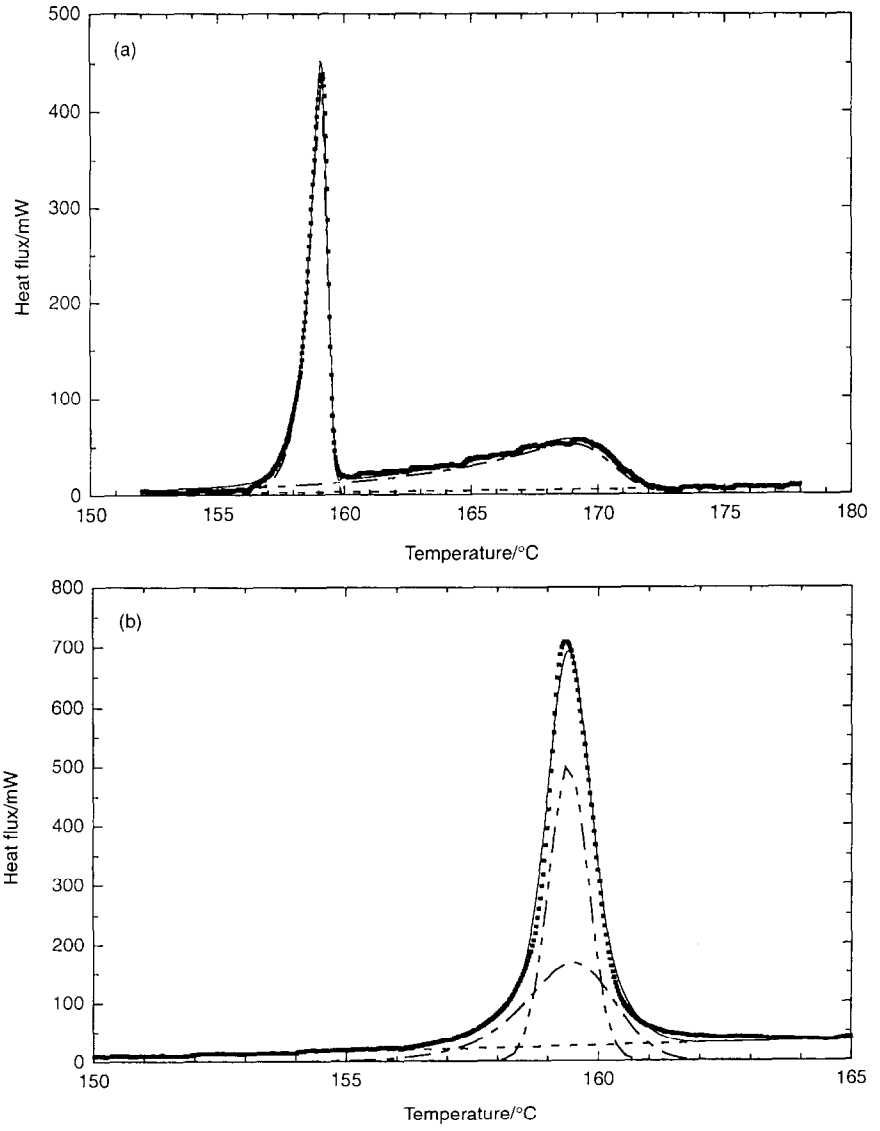

Fig. 1. (a, b)

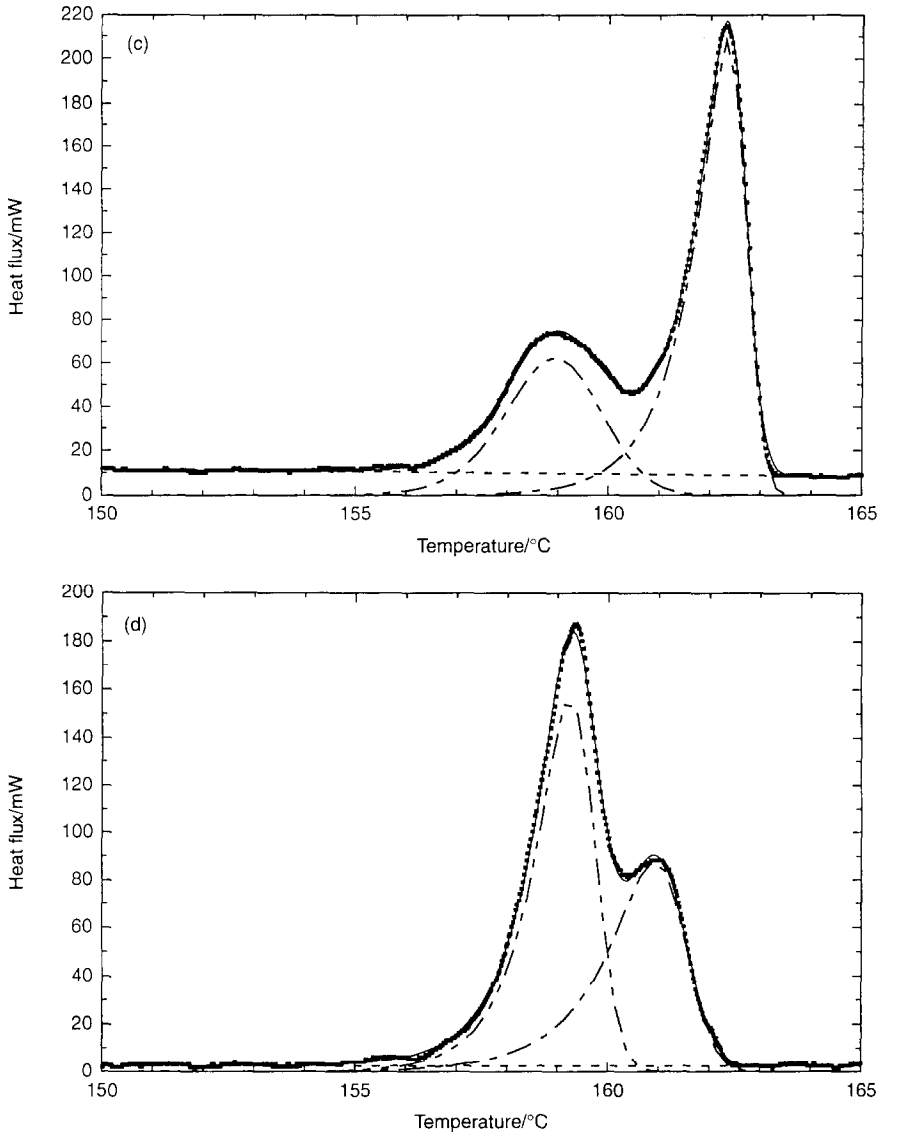

Fig. 1. Deconvoluted DSC plots of heat flux as a function of temperature for physical mixtures of (1S,2S)-(+)- and (1R,2R)-(−)-Ψ-ephedrine HCl. ■, Experimental points; ----, linear baseline; – – – – , and – – –, deconvoluted endotherms; ——, summation of deconvoluted endotherms and baseline. (a) 16.87 mol% (1S,2S)-(+)-Ψ-ephedrine HCl; (b) 29.81 mol% (1S,2S)-(+)-Ψ-ephedrine HCl; (c) 45.57 mol% (1S,2S)-(+)-Ψ-ephedrine HCl; (d) 59.76 mol% (1S,2S)-(+)-Ψ-ephedrine HCl.

(1S,2R)-(+)-ephedrine HCl [8]. In the present work, the melting point of the mixture decreased with decreasing mol% of one component to a minimum at about 60–72 mol%; then it increased to a maximum at 50 mol%. The rise in melting point indicates the formation of a racemic compound in this composition range (30–70 mol%). The

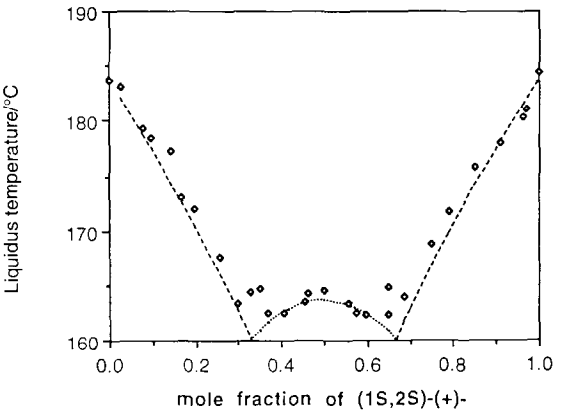

Fig. 2. Liquidus temperature phase diagram for the system (1S,2S)-(+)- and (1R,2R)-(−)-Ψ-ephedrine HCl: (– –) Schröder–van Laar equation; (· · · ·) Prigogine–Defay equation; (◇) experimental points.

experimentally obtained melting point phase diagram was compared with a theoretical curve from the Schröder–van Laar equation [11,12] outside the composition range between the eutectic points, i.e. 0–30 mol% and 70–100 mol%. In the composition range 30–70 mol%, the Prigogine–Defay equation [10] was used to calculate the theoretical curve. The experimental and calculated phase diagrams are given in Fig. 2. It can be seen that the points increasingly deviate from the theoretical lines as the composition is changed from 100 mol% to 70 mol% of either component, and the maximum deviation occurs near the intersection of the two theoretical curves. The eutectic points for the experimental plot in Fig. 2 are not clear, due to the deviant points near the eutectic composition. These deviations are to be expected from, (i) non-ideal behaviour and/or (ii) a change in ΔH_f^m, due to the finite heat capacity of the solid–liquid transition.

A clearer way of representing the solid–liquid phase behavior is by using the enthalpies of fusion for both endotherms at each composition. Fig. 3 shows plots of ΔH_f^m for the high (pure component or complex) and low melting endotherms as a function of composition. ΔH_f^m values were calculated for each peak from its area as a percentage of the total area (from Peakfit®) and the total enthalpy of fusion (from the DSC7 software). The phase diagram based on the ΔH_f^m values is also interpreted in terms of racemic compound formation, with eutectic points corresponding to mixing of the racemic compound with either of the enantiomers at 25.6 mol% and 69.4 mol% of (1S,2S)-(+)-Ψ-ephedrine HCl. These points are calculated from simultaneous solution of the regression coefficients for the lines intersecting at the eutectic and the theoretical 1 : 1 composition. Table 2 reports statistical data for these lines. As these calculated eutectic points should be symmetrically disposed about 50 mol% composition, the best estimates of the eutectic compositions from the present data are 28.1 ± 2.5 mol% and 71.9 ± 2.5 mol%.

Although DSC scans showed significant differences after the addition of even a small amount (1–2 mol%) of the minor enantiomer, the IR spectra did not display

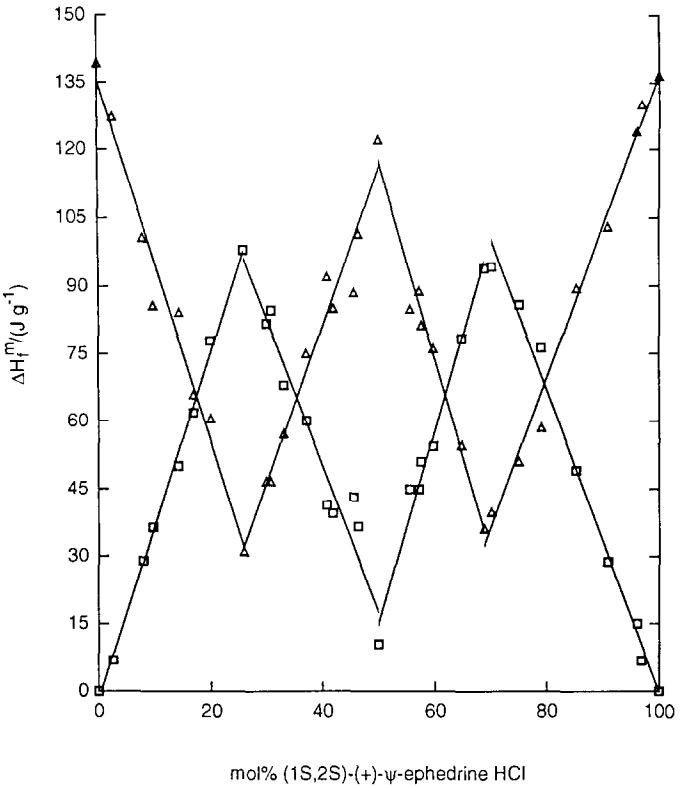

Fig. 3. Solid–liquid phase diagram for the system (1S,2S)-(+)- and (1R,2R)-(−)-Ψ-ephedrine HCl: △, ΔH_f^m values for the high melting endotherm (1); □, ΔH_f^m values for the low melting endotherm (2) as a function of composition.

large differences over the composition range from pure (1S,2S)-(+) enantiomer to the racemate. Small monotonic composition-dependent trends were seen in bands at 2936 (C–H stretch), 2735 (aminium N–H stretch) and 1428 (C–H bend adjacent to aminium) cm^{-1}, while other wavenumber changes were seen for bands at 3311 cm^{-1} (H-bonded O–H stretch) and 3010 cm^{-1} (H-bonded N–H stretch). Such wavenumber changes were often maximal near the eutectic composition. Side bands or shoulders on bands at 3010, 2936, 1455 (aromatic ring skeletal stretch), 1428 and 596 (aminium N–H deformation) cm^{-1} for the (1S,2S)-(+) enantiomer were progressively strengthened in compositions leading to the racemate. Small shoulders on bands at 2735 and 1076 (C–OH stretch) cm^{-1} in the enantiomer were absent in the racemate. These spectral changes largely involve bands associated with polar moieties and are expected to reflect differences in the H-bonding arrangements of the enantiomer and racemate. The phase diagram and the IR spectral changes again demonstrate clearly that grinding of the pure enantiomers in the solid state can result in a changed crystal structure [9]. An X-ray diffraction structure of crystalline (±)-Ψ-ephedrine HCl would be very helpful.

Table 2
Regression coefficients for the Ψ-ephedrine HCl solid–liquid phase diagram

Composition range/mol%	Intercept	Slope	Coefficient of variation (r^2)
Endotherm 1			
0–25.8	−1.749	3.8605	0.998
25.8–50	179.64	−3.2400	0.974
50–69	−197.79	4.2582	0.991
69–100	335.17	−3.3536	0.994
Endotherm 2			
0 25.8	135.42	−4.0123	0.981
25.8–50	−57.40	3.4671	0.969
50–69	333.69	−4.3310	0.987
69–100	−197.6	3.3421	0.995

3.2. Phase diagrams of (1S,2S)-(+)-Ψ-ephedrine HCl and (1S,2R)-(+)-ephedrine HCl

When 2–3 mol% of (1S,2R)-(+)-ephedrine HCl was ground with (1S,2S)-(+)-Ψ-ephedrine HCl, a second DSC endotherm appeared at a lower temperature (peak temperature, 154.8°C) than the principal endotherm (peak temperature, 216.5°C). On increasing the mol% of (1S,2R)-(+)-ephedrine HCl, the principal endotherm became very broad and overlapped with the minor endotherm. At approximately 70 mol% (1S,2S)-(+)-Ψ-ephedrine HCl, the two endotherms coalesced into one peak with a broad base. A second, very broad, endotherm began to appear at about 60 mol% (1S,2S)-(+)-Ψ-ephedrine HCl, which increased at the expense of the lower temperature endotherm. Near 10 mol% (1S,2S)-(+)-Ψ-ephedrine HCl, the two endotherms separated. In the composition range 10–93 mol% (1S,2S)-(+)-Ψ-ephedrine HCl, deconvolution of the two endotherms was necessary. The liquidus temperature phase diagram was unsymmetrical (Fig. 4). The Schröder–van Laar equation was used to calculate the melting points using the experimentally obtained values of ΔH_f^m for the pure components and the theoretical curve is also given in Fig. 4. Two experimental points deviated significantly from the theoretical lines near their intersection at 67 mol%.

The deconvoluted ΔH_f^m values for the two endotherms were also used to construct a phase diagram (Fig. 5). The diagram consists of upright and inverted triangles for $\Delta H_f^m(1)$ and $\Delta H_f^m(2)$, respectively. Each appears to have a plateau or shallow indentation at its apex, centered near 60 mol% of (1S,2S)-(+)-Ψ-ephedrine HCl. This suggested eutectic formation between each pure diastereomer and a weak complex that existed over the composition range 50–70 mol%. The phase diagram based on liquidus temperatures was not inconsistent with this interpretation. Table 3 contains the deconvoluted values of $\Delta H_f^m(1)$ and $\Delta H_f^m(2)$ and the measured liquidus temperatures. Because this system involves a pair of

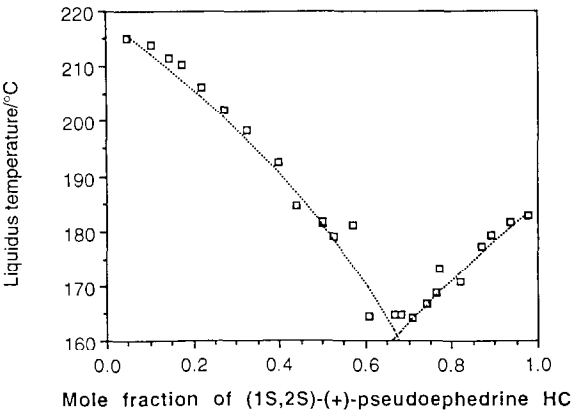

Fig. 4. Calculated (· · · ·) and experimental (□) liquidus temperatures as a function of composition in the (1S,2S)-(+)-Ψ-ephedrine HCl–(1S,2R)-(+)-ephedrine HCl system.

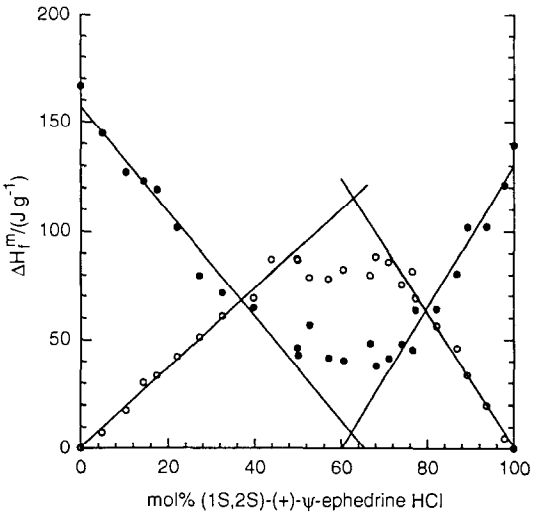

Fig. 5. Solid–liquid phase diagram for (1S,2R)-(+)-ephedrine HCl and (1S,2S)-(+)-Ψ-ephedrine HCl, plotting $\Delta H_f^m(1)$ (○) and $\Delta H_f^m(2)$ (●) as a function of composition. Regression equations and coefficients of variation (r^2) for the straight lines: $\Delta H_f^m(1) = 315.09 - 3.1469$ mol% (1S,2S) ($r^2 = 0.975$); $\Delta H_f^m(1) = -0.42654 + 1.8943$ mol% (1S,2S) ($r^2 = 0.987$); $\Delta H_f^m(2) = -196.12 + 3.2612$ mol% (1S,2S) ($r^2 = 0.956$); $\Delta H_f^m(2) = 159.76 - 2.6035$ mol% (1S,2S) ($r^2 = 0.971$).

isomers in a diastereomeric relationship, no racemic mixture is involved and the maxima and minima are at a composition not equal to 50%.

Simultaneous solution of the pairs of regression equations for $\Delta H_f^m(1)$ and $\Delta H_f^m(2)$ gave intersection points near to the mol% composition of the proposed weak complex, of 61.6 ± 1.1 mol% of the (1S,2S)-(+) isomer. These results imply that the complex is formed from three molecules of (1S,2S)-(+)-Ψ-ephedrine HCl

Table 3
Enthalpies of fusion and liquidus temperatures as a function of composition for the system (1S,2S)-(+)-Ψ-ephedrine HCl and (1S,2R)-(+)-ephedrine HCl

(1S,2S)-(+)-Ψ-ephedrine HCl/ mol%	$\Delta H_f^m(1)$/J g^{-1}	$\Delta H_f^m(2)$/J g^{-1}	Liquidus temperature/ °C
100.0	–	139.3	183.8
97.86	4.81	121.2	183.0
93.62	19.85	102.2	181.7
89.35	33.82	102.0	179.3
86.92	46.19	80.47	177.3
82.16	56.54	64.12	170.8
77.33	69.15	63.80	173.2
76.60	81.52	45.30	168.8
74.11	75.46	47.92	166.8
71.08	85.89	41.35	164.0
68.12	88.38	38.01	164.7
66.79	79.85	48.39	164.5
60.64	82.49	40.50	164.3
57.10	78.25	41.80	181.1
52.77	78.90	56.90	179.0
50.11	86.70	42.85	181.6
49.96	87.47	46.16	181.5
44.00	87.10	–	184.6
39.76	69.17	64.76	192.4
32.63	60.97	71.70	198.4
27.27	51.18	79.66	202.3
22.05	42.20	101.7	206.1
17.46	33.44	119.2	210.3
14.38	30.28	123.1	211.5
10.39	17.56	127.1	213.8
4.89	7.40	144.9	215.0
0.00	–	166.3	216.5

and two molecules of (1S,2R)-(+)-ephedrine HCl. If the complex does exist, the data could also be consistent with a 1:2 stoichiometric ratio, i.e. 66.7 mol% composition. Further experimental data in the composition range 40–80 mol% of the (1S,2S)-(+) isomer would be needed for a clearer interpretation of the phase diagram, including confirmation of the existence of the weak complex and its composition. Other techniques, such as X-ray diffraction and solid-state NMR spectra would be of value in confirming the existence of the complex.

4. Conclusions

A recent presentation of a regulatory perspective on chiral drugs emphasised the centrality of analytical controls for both stereochemical identity and purity [17]. The importance of methods for both stereochemical identification and quantitation

was recognised. The present study further supports earlier studies showing that DSC can easily detect minor contamination of an optically active drug by its antipode or by other closely related substances. It must be acknowledged that at present the method proposed is only suitable for drugs which melt without decomposition. The use of DSC, as discussed so far, does not provide direct evidence for stereochemical identity. However, stereochemical identification of an enantiomer can be achieved with DSC by scanning the unknown enantiomer in admixture with an equal amount of a reference sample of either of the pure enantiomers. This is a much more sophisticated form of the "mixed melting point test" of classical organic chemistry. The mixture with the same enantiomer will give a scan which should be identical to the unknown alone, while the mixture with the antipode will lead to a more complex scan (additional endotherms, a different enthalpy of fusion or a different shaped endotherm). The method is expected to fail in the rare case of racemic solid solution formation [9].

The study further demonstrates the utility of deconvolution software, such as PeakFit®, for separating overlapping DSC endotherms. This allows quantitation of stereochemical purity. The approach could also be used in deconvoluting heat flux changes due to thermal events such as polymorphic transitions or chemical degradation which overlap with melting endotherms. This may allow the method to be extended to drugs which do not melt cleanly. The present research demonstrates two further clear examples where enthalpy of fusion values from deconvoluted endotherms can be used to simplify the analysis of a solid–liquid phase diagram.

Acknowledgments

Experimental data for the research described in this paper was obtained in the Department of Pharmaceutics, University of Florida (Gainesville, FL), and was funded by a University of Florida DSR Research Development Award. Additional financial support was given by SmithKline Beecham Pharmaceuticals (King of Prussia, PA).

Appendix: Equations

The Schröder–van Laar equation is

$$-\ln x_1 = \frac{\Delta H_f^m}{R}\left(\frac{1}{T} - \frac{1}{T_1^\circ}\right)$$

where T_1° is the liquidus temperature of the pure enantiomer, ΔH_f^m is the enthalpy of fusion of the pure enantiomer, x_1 is the mole fraction of the enantiomer in excess and T is the liquidus temperature for any given composition.

The Prigogine–Defay equation is

$$\frac{\Delta H_f^m}{R}\left(\frac{1}{T} - \frac{1}{T_c}\right) = -\ln x_2(1 - x_2) + \ln 0.25$$

where T_c is the liquidus temperature of the racemic compound and ΔH_f^m is the enthalpy of fusion of the racemic compound.

References

[1] T. Kansawa, Bull. Chem. Soc. Jpn., 29 (1956) 398, 479.
[2] J.B. Hyne, Can. J. Chem., 38 (1960) 125.
[3] J.B. Hyne, Can. J. Chem., 39 (1961) 2536.
[4] P.S. Portoghese, J. Med. Chem., 10 (1967) 1057.
[5] R. Bergin, Acta Crystallogr. Sect. B, 27 (1971) 381.
[6] M. Mathew and G.J. Palenik, Acta Crystallogr. Sect. B, 33 (1977) 1016.
[7] W.F. Schmidt, W. Porter and J.T. Carstensen, Pharm. Res., 5 (1988) 391.
[8] M.Z. Elsabee and R.J. Prankerd, Int. J. Pharm., 86 (1992) 211.
[9] M.Z. Elsabee and R.J. Prankerd, Int. J. Pharm., 86 (1992) 221.
[10] I. Prigogine and R. Defay, translated by D.H. Everett, Chemical Thermodynamics, Longmans, London, 1954.
[11] I. Schröder, Z. Phys. Chem., 11 (1893) 449.
[12] J.J. van Laar, Arch. Néerl II, 8 (1903) 264; cited in Ref. [10], p. 358.
[13] H. Downes, R.S. Perry, R.E. Ostlund and R. Karler, J. Pharmacol. Exp. Ther., 175 (1970) 692.
[14] K.C. Rice, J. Org. Chem., 47 (1982) 3617.
[15] S.P. Duddu, R. Mehvar and D.J.W. Grant, Pharm. Res., 8 (1991) 1430.
[16] S.P. Duddu, F.K.-Y. Fung and D.J.W. Grant, Int. J. Pharm., 94 (1993) 171.
[17] W.H. De Camp, in D.J.A. Crommelin and K.K. Midha (Eds.), Topics in Pharmaceutical Sciences 1991, Medpharm, Stuttgart, 1992, Chap. 25.